Redox Chemistry and Spectroscopy of Toluene-3,4-dithiol ($TDTH_2$) and of Its $M(TDT)_2^{2-/-}$ Complexes with Zinc(II), Copper(II), Nickel(II), Cobalt(II), Iron(II), and Manganese(II). Formation of a Stable d^n-(·SR) Bond upon Oxidation by One Electron

Donald T. Sawyer,*† G. Susan Srivatsa, Mario E. Bodini,‡ William P. Schaefer,§ and Richard M. Wing

Contribution from the Department of Chemistry, University of California, Riverside, California 92521. *Received June 28, 1985*

Abstract: In aprotic media, the anion of toluene-3,4-dithiol ($TDTH_2$) is oxidized at −0.05 V vs. SCE to a disulfide dimer $H_2(TDT)_2$ by an irreversible one-electron process. The combination of its dianion (TDT^{2-}) with divalent transition metals, M(II) (where M = Zn, Cu, Ni, Co, Fe, and Mn), in a two-to-one mole ratio yields stable complexes $[M^{II}(TDT)_2]^{2-}$. Upon exposure to air these are rapidly oxidized to yield monoanionic species $[M(TDT)_2]^-$. The site of electron transfer for the oxidation of $[M(TDT)_2]^{2-}$ to $M(TDT)_2^-$ has been assigned to a bound sulfide group which spin pairs with an unpaired d electron of the transition metal to yield a stable covalent bond on the basis of the observed redox potentials, optical spectra, and magnetic properties. The monoanions, $[M(TDT)_2]^-$, display intense visible absorption bands that are assigned to the excitation of the M^{II}-(·TDT) bond. The structures for the $[Cu(TDT)_2][Bu_4N]$ and $[Fe(TDT)_2]_2[Bu_4N]_2$ complexes have been determined by single-crystal X-ray diffractometry. The monomeric copper complex has a copper(II) center surrounded by an essentially square-planar array of four sulfur atoms from two TDT ligands with an average Cu–S bond distance of 2.164 (12) Å. The iron complex is a dimer which contains the iron atom in a distorted square-pyramidal environment of sulfur atoms with average in-plane Fe–S distances of 2.221 (6) Å. A sulfur atom from an ion across an inversion center occupies an axial position 2.513 (5) Å from the iron atom.

The toluene-3,4-dithiolate complexes of transition-metal ions were first studied more than 50 years ago.[1,2] Subsequent work was directed to the use of toluene-3,4-dithiol ($TDTH_2$) as an analytical reagent[3,4] and to structural characterizations of metal–dithiolate complexes.[5]

The diversity of structural types with variant nuclearity,[6-8] the utility of certain complexes as precursors to new clusters and cages,[9,10] and the ability of certain coordinately-saturated metal–sulfur complexes to serve as simple models of the active sites for metal–sulfide heterogeneous catalysts[11] have prompted numerous investigations of transition-metal thiolate chemistry. In addition, metal–thiolate complexes are known to form unique one-dimensional systems[12,13] and donor–acceptor complexes.[14,15] Transition-metal dithiolate complexes also have attracted the attention of bioinorganic chemists because of the common occurrence of metal–sulfur bonding in biological systems.[16-19]

Metals with sulfur donors (either a thiolate from a cysteine residue or a thioether linkage from a methionine residue) are found in iron–sulfur proteins[17] (ferredoxins, nitrogenase), blue-copper proteins[19] (plastocyanin, stellacyanin, azurin), molybdo proteins[17] (nitrogenase, xanthine oxidase), and liver alcohol dehydrogenase (Zn–S).

Previous papers from our group have been concerned with the redox properties of 3,5-di-*tert*-butylcatechol ($DTBCH_2$) and its semiquinone and quinone in aprotic media.[20] The structural and redox chemistry of the semiquinonato and catecholato complexes of iron,[21,22] chromium,[21,23] vanadium,[23-26] manganese,[27] zinc,[28] and copper[29] also have been described. For all of these metal–catechol complexes, the redox chemistry is ligand-based, and the metal–redox chemistry occurs via electron transfer to and from the ligand. Because *o*-benzodithiols represent sulfur analogues to catechols, they are expected to have similar coordination chemistry but to be subject to more extensive redox processes.

Toluene-3,4-dithiol forms strong bis complexes with divalent metals, $[M^{II}(TDT)_2]^{2-}$, and all of these, except the Zn(II) complex, are oxidized easily by air to form more stable $[M(TDT)_2]^-$ species. This oxidation has been thought to be metal centered to give a

† Present address: Department of Chemistry, Texas A&M University, College Station, Texas, 77843.
‡ Chemistry Faculty, Catholic University of Chile, Santiago, Chile.
§ Department of Chemistry and Chemical Engineering, California Institute of Technology, Pasadena, California, 91125.

(1) Mills, W. H.; Clark, R. E. D. D. *J. Chem. Soc.* **1936**, 175.
(2) Clark, R. E. D. *Analyst (London)* **1936**, *60*, 242; **1937**, *62*, 661.
(3) Hamence, J. *Analyst (London)* **1940**, *65*, 151. Miller, C. C.; Lowe, A. J. *J. Am. Chem. Soc.* **1940**, 1258. Wells, J. E.; Pemberton, R. *Analyst (London)* **1947**, *72*, 185.
(4) Short, H. G. *Analyst (London)* **1951**, *76*, 710.
(5) McCleaverty, J. A. *Prog. Inorg. Chem.* **1968**, *10*, 50.
(6) Tremel, W.; Krebs, B.; Hinkel, G. *Agnew. Chem., Int. Ed. Engl.* **1984**, *23*, 634.
(7) Gaite, W.; Ros, J.; Solans; X.; Font-Altoba, M.; Brianso, J. L. *Inorg. Chem.* **1984**, *23*, 39.
(8) Dorfman, J. R.; Holm, R. H. *Inorg. Chem.* **1983**, *22*, 3179.
(9) Choy, A.; Craig, D.; Dance, I.; Scudder, M. J. *J. Chem. Soc., Chem. Commun.* **1982**, 1246.
(10) Dance, I. G.; Choy, A.; Scudder, M. L. *J. Am. Chem. Soc.* **1984**, *106*, 6285.
(11) Millar, M.; Koch, S. International Conference on Coordination Chemistry, Abstract Mn 5-6, Boulder, Colorado, 1984.
(12) Interrante, L. V., Ed. "Extended Interactions Between Metal Ions in Transition Metal Complexes"; American Chemical Society: Washington, D.C., 1974; American Chemical Society Symposium Series, No. 5.
(13) Hatfield, W. E. "Molecular Models", NATO Conference Series, Plenum Press: New York, 1979; Vol. I, Series VI.
(14) Manoharan, P. T.; Noordik, J. H.; de Boer, E.; Keijzers, C. P. *J. Chem. Phys.* **1981**, *74*, 1980.
(15) Valade, L.; Bousseau, M.; Gleizes, A.; Cassoux, P. *J. Chem. Soc., Chem. Commun.* **1983**, 110.
(16) Lawrence, G. D.; Sawyer, D. T. *Coord. Chem. Rev.* **1978**, *27*, 173.
(17) Spiro, T. G., Ed. "Iron Sulfur Proteins"; John Wiley and Sons, Inc.: New York, 1982; Vol. 4.
(18) Cammack, R.; Christou, G. In "Hydrogenases: Their Catalytic Activity, Structure, and Function"; Schlegal H. G., Schneider, K. Eds., Verlag Erich Goltze KG: Göttingen, 1978; pp 45–56.
(19) Siegel, H., Ed. "Copper Proteins"; Marcel Dekker, Inc.: New York, 1981; Vol. 13.
(20) Stallings, M. D; Morrison, M. M.; Sawyer, D. T. *Inorg. Chem.* **1981**, *20*, 2655.
(21) Buchanan, R. M.; Kessel, S. L.; Downs, H. H.; Pierpont, C. G.; Hendrickson, D. N. *J. Am. Chem. Soc.* **1978**, *100*, 7894.
(22) Jones, S. E.; Leon, L. E.; Sawyer, D. T. *Inorg. Chem.* **1982**, *21*, 3692.
(23) Downs, H. H.; Buchanan, R. M.; Pierpont, C. G. *Inorg. Chem.* **1979**, *18*, 1736.
(24) Bosserman, P. J.; Sawyer, D. T. *Inorg. Chem.* **1982**, *21*, 1545.

0002-7863/86/1508-0936$01.50/0 © 1986 American Chemical Society

trivalent metal–dithiolate complex $[M^{III}(TDT)_2]^-$. Although the structural aspects of these complexes have been discussed,[5] their redox chemistry is not as well-characterized and may be important to an understanding of the role of the sulfur atom in the overall chemistry of these complexes.

The present study describes the redox chemistry of toluene-3,4-dithiol ($TDTH_2$) and of its complexes with the divalent ions of Zn, Cu, Ni, Co, Fe, and Mn in aprotic media. Specifically, the question of the site of electron transfer in the oxidation of $[M^{II}(TDT)_2]^{2-}$ to $[M(TDT)_2]^-$ has been addressed. The structures for the monomeric $[Cu(TDT)_2][Bu_4N]$ and dimeric $[Fe(TDT)_2]_2[Bu_4N]_2$ complexes also have been determined by single-crystal X-ray diffraction measurements.

Experimental Section

Equipment. The cyclic voltammetry and controlled-potential electrolysis were accomplished with a three-electrode potentiostat (Princeton Applied Research Model 173 potentiostat/galvanostat, Model 175 Universal programmer, and Model 179 digital coulometer) and Houston Instruments Model 100 Omnigraphic X–Y recorder. The electrochemical measurements were made with a Bioanalytical Systems microcell assembly (10-mL capacity) that was adapted to use a platinum-inlay working electrode (area, 0.033 cm^2), a platinum-wire auxiliary electrode, and an Ag/AgCl reference electrode (filled with aqueous tetramethylammonium chloride solution and adjusted to 0.000 V vs. SCE)[30] with a solution junction via a glass tube closed with a cracked-glass bead that was contained in a luggin capillary. A platinum-flag auxiliary electrode (contained in a glass tube with medium porosity glass frit and filled with a concentrated solution of supporting electrolyte) and a platinum-mesh working electrode were used for controlled potential electrolysis.

The UV–visible spectrophotometric measurements were made with a Cary Model 219 spectrophotometer.

The ESR spectra were recorded on a Bruker Model ER 200D ESR spectrometer with a 12-in. magnet. The spectra at 77 K were obtained by use of a small, quartz liquid-nitrogen finger dewar. Room-temperature spectra were recorded with samples in melting-point capillaries, which were placed inside a standard ESR tube. Magnetic susceptibilities of solids were measured by the Gouy Method, and the solution magnetic susceptibilities were determined by the Evans' method.[31] Temperature-dependent magnetic susceptibility measurements were made with a variable-temperature superconducting susceptometer/magnetometer (SHE Corporation, Model 905/2K/H/868; 5 T field).[32] Air-sensitive compounds were synthesized and handled inside a Vacuum Atmospheres drybox (Model HE-43-2 Drilab with a Model He-193-1 Dritrain) under a nitrogen atmosphere.

Chemicals and Reagents. Acetonitrile (AN), dimethyl sulfoxide (Me_2SO_4), methylene chloride (CH_2Cl_2) (Burdick and Jackson Laboratories, "distilled in glass" grade), toluene (Mallinckrodt), tetraethylammonium perchlorate) (TEAP, G. Frederick Smith), and toluene-3,4-dithiol ($TDTH_2$, Eastman Kodak) were used without further purification. The source of divalent metals was $CuCl_2{\cdot}2H_2O$, $NiCl_2{\cdot}6H_2O$, and $CoCl_2{\cdot}6H_2O$ (Mallinckrodt). Tetrakisacetonitrile perchloreate salts of Mn(II), Fe(II), and Zn(II) were synthesized by recrystallization of the hydrated perchlorate salts (Mallinckrodt) from acetonitrile.

Synthesis of Complexes. The $[Bu_4N][M(TDT)_2]$ complexes of Cu(II), Ni(II), Co(II), and Fe(II) were synthesized by previously published methods.[35] In situ generation of $[Zn^{II}(TDT)_2]^{2-}$ was accomplished by the combination of the divalent tetrakisacetonitrile perchlorate salt, $Zn^{II}(CH_3CN)_4(ClO_4)_2$, with 2TDTH and 4TEA(OH). In the presence of oxygen, the $[Zn^{II}(TDT)_2]^{2-}$ complex was stable to oxidation. The electrochemistry and the optical spectra for the chemically synthesized dithiolate complexes of Cu(II), Ni(II), Co(II), and Fe(II) were identical with those for the in situ generated species. The dianions, $[M^{II}(TDT)_2]^{2-}$, were generated by the electrochemical reduction of the chemically synthesized monoanions, $[M(TDT)_2]^-$, inside a Vacuum Atmospheres glovebox.

Crystallization of $[Cu(TDT)_2][Bu_4N]$ and $[Fe(TDT)_2]_2[Bu_4N]_2$. About 100 mg of crude material was dissolved in 40 mL of CH_2Cl_2 inside the drybox. To this was added 10 mL of toluene, and the solution was allowed to evaporate slowly through a glass wool plug. Both solvents had been passed through a bed of activated alumina (Woelm Super-1) inside the drybox to remove residual H_2O and any oxidized impurities. After complete evaporation of CH_2Cl_2, the single crystals that were suspended in toluene were carefully recovered by use of a disposable pipet and deposited onto a filter paper. The dry crystals were then removed from the drybox and stored in the absence of light.

X-ray Crystallography. $[Cu(TDT)_2][Bu_4N]$. Table I summarizes the crystal data and the collection conditions for the $(n\text{-}Bu_4N)[Cu(TDT)_2]$ salt. Room-temperature X-ray photographic data showed the crystal to be monoclinic. Systematic extinctions were consistent with space group $C2/c$ data reduction, and structure solution/refinement was accomplished by use of the Enraf–Nonius structure-analysis programs SDP PLUS version 1.0. An empirical absorption correction based on a ψ scan of the s1–4 reflection was applied to all of the data ($0.88 \leq$ transmission ≤ 1.0).

The square-planar $Cu(TDT)_2$ unit was disordered in such a way that the methyl group appeared at half occupancy at the toluene 6 as well as 1 positions. This precluded a definitive structural determination to confirm the presence of an electron-localized radical sulfur at one of the four-square coordination sites of the copper ion. For this reason, a restrained refinment procedure[33,34] was used. In spite of these difficulties the data confirm that the complex is monomeric and approximately square-planar.

$[Fe(TDT)_2]_2[Bu_4N]_2$. A summary of crystal data and the collection conditions for the dimeric $[Fe(TDT)_2]_2^{2-}$ complex are presented in Table

Table I. Crystal Data and Collection Conditions for $[n\text{-}Bu_4N][Cu(TDT)_2]$ and $[n\text{-}Bu_4N]_2[Fe(TDT)_2]_2$

	Cu	Fe
formula	$CuS_4C_{30}H_{46}N$	$(FeS_4C_{30}H_{46}N)_2$
space group	$C2/c$ (No. 15)	$P2_1/n$ (no. 14)
M_f (daltons)	613.53	2 × 606.83
a	42.510 (8) Å	14.985 (4) Å
b	8.586 (2) Å	14.148 (4) Å
c	18.716 (7) Å	17.133 (5) Å
β	105.49 (2)°	111.61 (2)°
V	6583 Å^3	3377 (2) Å
z	8	2
d_{calcd}	1.217 g cm^{-3}	1.19 g cm^{-3}
d_{obsd}[a]	1.210 g cm^{-3}	
cryst dimens	0.3 × 0.1 × 0.1 mm (cut from 5 × 3 × 0.1 mm plate)	0.04 × 0.13 × 0.14 mm dark
cryst color	emerald green	
diffractometer	CAD-4 Enraf–Nonius	Syntex $P2_1$
radiatn	graphite monochromatized Mo Kα	(λ, 0.7107 Å)
scan type	$\omega/2\theta$	$\omega/2\theta$
scan width	1° + 0.35 tan θ	2° + dispersion
unique data	2068	1370
$I > 3\sigma(I)$	1172	832
no. of variables	103	176
R[b]	0.084	0.092
R_ω[c]	0.076	
esd[d]	2.4	1.68
larg param shift	0.25 × its esd	0.19 × its esd
larg peak in difference map[e]	0.35 e Å^{-3}	1.99 e Å^{-3}, near Fe

[a] By flotation. [b] $R = \sum||F_o| - |F_c||/\sum|F_o|$. [c] $R_\omega = [\sum\omega(||F_o| - |F_c||)^2/\sum\omega/F_o^2]^{1/2}$ and $\omega = (4F^2)/L^2\sigma(I))$ where L is the reciprocal Lorentz polarization factor and $\sigma(I) = [P + 4B + 0.045\ I^2]^{1/2}$. Here P equals the total counts collected during the scan, and B equals the background counts. [d] From the final refinement cycle; standard deviation of an observation of unit weight. [e] From final difference Fourier.

(25) Cooper, S. R.; Koh, Y. B.; Raymond, K. N. *J. Am. Chem. Soc.* **1982**, *u04*, 5092.
(26) Cass, M. E.; Green, D. L.; Buchanan, R. M.; Pierpont, C. G. *J. Am. Chem. Soc.*, in press.
(27) Chin, D.-H.; Sawyer, D. T.; Schaefer, W. P.; Simmons, C. J. *Inorg. Chem.* **1983**, *22*, 752.
(28) Bodini, M. E.; Copia, G.; Robinson, R.; Sawyer, D. T. *Inorg. Chem.* **1983**, *22*, 126.
(29) Harmalker, S.; Jones, S. E.; Sawyer, D. T. *Inorg. Chem.* **1983**, *22*, 2791.
(30) Chin, D.-H.; Chiercato, G., Jr.; Nanni, E. J., Jr.; Sawyer, D. T. *J. Am. Chem. Soc.* **1982**, *104*, 1296.
(31) Evans, D. F. *J. Chem. Soc.* **1959**, 2003.
(32) NSF Regional SQUID Magnetometer Facility, Department of Chemistry, University of Southern California, Los Angeles, CA.
(33) Flippen-Anderson, J. L.; Konnert, J. H.; Gilardi, R. *Acta Crystallogr., Sect. B: Struct. Sci.* **1982**, *B38*, 2865.
(34) Parameters used in the restrained refinement: (a) $(n\text{-butyl})_4N$; C–C = 1.54 Å, C–N = 1.47 Å, all angles = 109.5°. (b) toluene-3,4-dithiol ligands; C–C aromatic = 1.390 Å, C–CH_3 = 1.465 Å, C–S = 1.735 Å, all angles = 120.0°. The final parameters had a mean esd of ±0.08 Å from the above values.

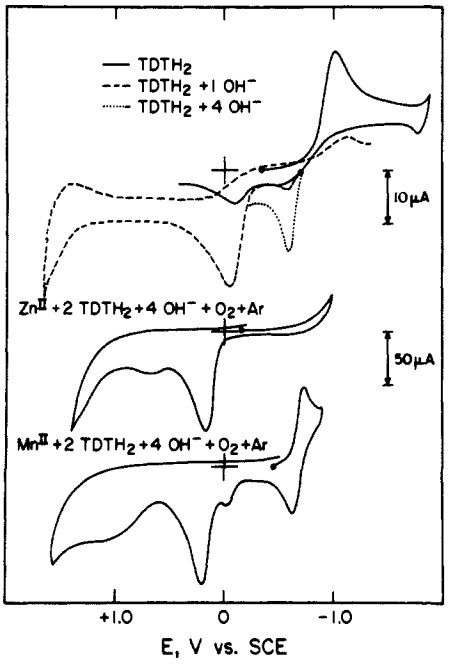

Figure 1. Cyclic voltammograms in MeCN (0.1 M TEAP) of (a, top) 3.7 mM toluene-3,4-dithiol, $TDTH_2$ (solid line), 3.7 mM $TDTH^-$ from combination of $TDTH_2$ and 1 equiv of tetraethylammonium hydroxide [TEA(OH)] (dashed line), and 3.7 mM $TDTH^-$ plus 11 mM OH^- [combination of $TDTH_2$ and 4 equiv of TEA(OH)] (dotted line), (b, middle) 9.7 mM $[Zn(TDT)_2]^{2-}$ from the combination of one $Zn^{II}(ClO_4)_2 \cdot 4MeCN$ plus $2TDTH_2$ and 4TEA(OH), and (c, bottom) 5.2 mM $[Mn(TDT)_2]^-$ from the combination of $1Mn^{II}(ClO_4)_2$ plus $2TDTH_2$ and 4TEA(OH) in the presence of O_2. Scan rate, 0.1 V s^{-1}; Pt electrode surface area, 0.11 cm^2.

I. Unit-cell dimensions were obtained from the setting angles of 15 reflections with $16° < 2\theta < 20°$. Space group $P2_1/n$, a special setting of #14 with equivalent positions $\pm(x, y, z, {}^1/_2 + x, {}^1/_2 - y, {}^1/_2 + z)$, was chosen based on the systematic absences $h0l$, $h + l = 2n + 1$, and $0k0$, and $k = 2n + 1$, in the intensity data. The crystal did not diffract strongly at high angles, so data were collected only to $2\theta = 30°$. Refinement minimized $w(F_o^2 - F_c^2)^2$, where $w = 1/\sigma^2(F_o^2)$. Variances were assigned to the individual values of F_o^2 based on counting statistics plus an additional term $(0.014F_o^2)^2$ to account for errors proportional to intensity. Variances of the merged data were calculated by standard propagation of error plus another additional term, $(0.014\bar{F}_o^2)^2$. The final refinement included all 176 parameters in one matrix: positional parameters for all non-hydroen atoms, anisotropic thermal parameters for the iron and sulfur atoms, isotropic thermal parameters for the benzene ring carbon atoms and the atoms of the tetra-*n*-butylammonium ion, a scale factor, and two population parameters for the toluene methyl groups (disordered between their two possible positions). All hydrogen atoms were included at calculated positions and with arbitrary thermal parameters chosen to roughly match the carbon atom to which they are bonded. They were repositioned four times during the refinement, which converged after 24 cycles with $R = \sum||F_o| - |F_c||/\sum F_o = 0.092$ for the 1198 reflections with $F_o^2 > 0$ and 0.062 for the 832 reflections with $F_o^2 > 3\sigma(F_o^2)$.

The toluene methyl groups occupy a major and a minor state on both thiolate groups. The thermal and the population parameters of the methyl carbons could not both be refined together, so for the final cycles the thermal parameters B of the four methyl carbon atoms were fixed at 15.0 $Å^2$, a value close to what three of them had refined to earlier. The population parameters of the major sites then refined to 0.78 (2) (C(7A), attached to C(4)) and 0.62 (2) (C(14A), attached to C(11)). C(7B), attached to C(5), had population 1–0.78 and C(14B), attached to C(12), had population 1–0.62. Hydrogen atoms on these methyl groups were positioned with a hydrogen atom in the benzene ring plane pointing away from the alternate methyl position and the other two hydrogen atoms at tetrahedral angles; they were given the same population as the carbon atoms.

Results

Electrochemistry. Figure 1a illustrates the electrochemical reduction and oxidation of toluene-3,4-dithiol ($TDTH_2$) and its anion ($TDTH^-$). With the addition of excess OH^- the small anodic peak at –0.60 V vs. SCE for TDT^{2-} becomes a full one-electron oxidation peak. Controlled potential coulometry confirms that the oxidation and reduction of $TDTH_2$ are one-electron processes; the reduction yields $TDTH^-$. The oxidation of the latter species yields a neutral product that has a small proton-reduction peak at the same potential as $TDTH_2$ (–1.10 V vs. SCE).

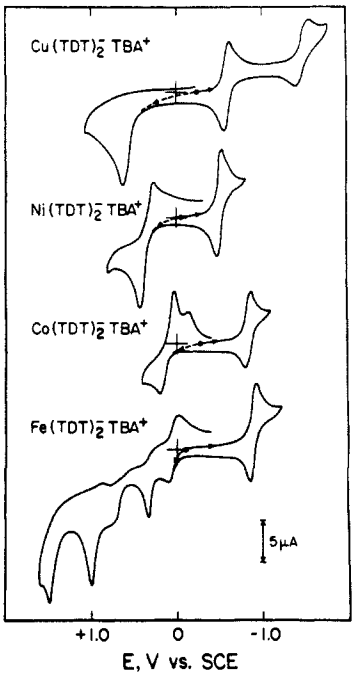

Figure 2. Cyclic voltammograms in MeCN (0.1 M TEAP) of $[M(TDT)_2][Bu_4N]$ complexes (M = Cu, Ni, Co, and Fe). Scan rate 0.1 V s^{-1}; Pt electrode surface area, 0.11 cm^2.

The addition of Zn(II) to a dithiolate solution [$2TDTH_2$ + $4OH^-$] results in the formation of the bisdithiolate complex, $[Zn^{II}(TDT)_2]^{2-}$ (Figure 1b), which is stable to air oxidation. Other mole ratios yield a mixture of free Zn(II) and/or free ligand in addition to the stable complex. Similar to the free ligand, the zinc dithiolate complex, $[Zn^{II}(TDT)_2]^{2-}$, is irreversibly oxidized at +0.18 V vs. SCE (Figure 1b). The addition of manganese(II) to a dithiolate solution in the presence of air yields a product that gives the cyclic voltammogram shown in Figure 1c. The $[Mn^{II}(TDT)_2]^{2-}$ complex that is initially formed is oxidized by molecular oxygen to yield $[Mn(TDT)_2]^-$. The $[Mn^{II}(TDT)_2]^{2-}/[Mn(TDT)_2]^-$ redox couple is reversibe ($E_{1/2}$ = –0.67 V vs. SCE); the $[Mn(TDT)_2]^-$ complex is oxidized irreversibly at +0.22 V. The small anodic peak at –0.05 V (Figure 1c) is due to excess ligand ($TDTH^-$) in the solution.

Figure 2 illustrates the cyclic voltammograms for the chemically synthesized $[M(TDT)_2]^-$ complexes of Cu(II), Ni(II), Co(II), and Fe(II) in acetonitrile. The electrochemistry, spectroscopy, and magnetic properties of the metal–dithiolate complexes generated in situ by the addition of M(II) to ($2TDTH_2 + 4OH^-$) are identical with those for the one-electron reduction products of synthesized complexes, $[Bu_4N][M(TDT)_2]$. The cyclic voltammograms for the monoanionic metal–dithiolate complexes exhibit a reversible reduction couple between –0.5 and –1.0 V vs. SCE. The $[Cu(TDT)_2]^-$ complex exhibits a second reversible reduction at –1.5 V vs. SCE.

The anodic electrochemistry for $[Cu(TDT)_2]^-$ is similar to that for the $[Mn(TDT)_2]^-$ complex with an irreversible oxidation at +0.62 V. The cyclic voltammograms for $[Co(TDT)_2]^-$ and $[Ni(TDT)_2]^-$ exhibit single, quasi-reversible oxidations at +0.20 and +0.44 V, respectively. The $[Fe(TDT)_2]^-$ complex yields several oxidation peaks in the range from 0 to +1.5 V vs. SCE. The first two appear to be reversible and are one-electron-per-dimer oxidation steps on the basis of controlled potential coulometry. All of the $[M(TDT)_2]^-$ complexes exhibit an irreversible oxidation at +1.6 V, which upon scan reversal results in a reduction peak at the same potential as that for the reduction of the mo-

Table II. Electrochemical Oxidation Potentials for $M^{II}(TDT)_2^{2-}$ and $M^{II}Cl_4^{2-}$ Complexes in MeCN (0.1 M TEAP)

metal (M)	$E_{p,a}$, V vs. SCE $[M^{II}(TDT)_2]^{2-}$, 1 mM first oxidn	second oxidn		$[M^{II}Cl_4]^{2-}$, 1 mM
	(TDTH$^-$) −0.05 (irrev)		(Cl$^-$)	+0.95 (irrev)
Zn	+0.18 (irrev)			+1.10 (irrev)
Cu	−0.53	+0.62		+0.95 (irrev)
Ni	−0.47	+0.44		+1.12 (irrev)
Co	−0.73	+0.20		+0.5 (irrev)
Fe	−0.83	+0.10, +0.32		+0.10
Mn	−0.63	+0.22 (irrev)		+1.05 (irrev)

Table III. UV–vis Absorption Spectra and Spin States for the Bis(3,4-toluenedithiolate) Complexes of Divalent Metal Ions and Their One-Electron Oxidation Products in Acetonitrile[f]

metal (M)	$[M^{II}(TDT)_2]^{2-}$ λ (ε), nm (mM^{-1} cm^{-1})	spin state, (S)[a]	$[M^{II}(TDT)_2]^-$ λ (ε), nm (mM^{-1} cm^{-1})	spin state, (S)[a,e]
$TDTH_2$	220 (23.8)	0		
	296 (1.7)			
$TDTH^-$	240 (18.7)	0		
	294 (10.5)			
	330 (3.1)			
$H_2(TDT)_2$	238 (25.1)	0		
	294 (3.4)			
	330 (2.0)			
Cu	256 (66.6)	$^1/_2$[b]	239 (60.9)	0
	346 (11.5)		325 (10.8)	
	388 (9.65)		395 (32.0)	
	465 (5.43)		1236	
Ni	247 (37.6)	$^2/_2$[c]	247 (41.2)	$^1/_2$
	306 (23.8)		312 (24.8)	
	397 (5.62)		359 (9.7)	
	512 (0.76)		860 (9.4)	
Co	251 (44.0)	$^3/_2$[c]	245 (49.3)	$^2/_2$
	312 (15.2)		316 (12.7)	
	366 (7.35)		361 (13.7)	
	660 (1.20)		660 (12.0)	
Fe	248 (51.6)	$^4/_2$[c]	245 (43.3)	$^3/_2$
	328 (11.8)		315 (13.5)	
	355 (13.0)		370 (12.0)	
			526 (6.7)	
Mn		$^5/_2$[d]	242 (30.0)	$^4/_2$
			363 (11.1)	
			510 (2.3)	
			576 (1.9)	
			734 (1.51)	

[a] By Evan's method. [b] EPR results indicate an $S = {}^1/_2$ system. [c] Predicted spin states. [d] Data from ref 36. [e] On the basis of magnetic moment data from Table V. [f] Data are included for the ligand and its oxidation product $H_2(TDT)_2$.

noanions, $[M(TDT)_2]^-$, but with approximately four-to-eight times the current of the original reduction. Scan reversal after the latter reduction results in the original reversible redox couple.

Table II lists the oxidation potentials for the $[M^{II}(TDT)_2]^{2-}$ complexes as well as those for the analogous $(M^{II}Cl_4)^{2-}$ complexes. For each of these tetrachloro complexes except $(Fe^{II}Cl_4)^{2-}$ the initial anodic peak occurs at about +1.0 V vs. SCE and represents oxidation of a bound chloride ion. The $(Fe^{II}Cl_4)^{2-}$ complex has a reversible redox couple at +0.1 V vs. SCE, which is due to oxidation of the metal center.

Optical Spectroscopy. Table III summarizes UV–vis spectral data for $TDTH_2$, $TDTH^-$, and the product species from the one-electron oxidation of $TDTH^-$. As the charge density is increased, the major $\pi-\pi^*$ absorption band shifts to longer wavelengths. The coincidence of this band for the $TDTH^-$ oxidation product with that for $TDTH_2$ is consistent with the formation of a neutral disulfide $[H_2(TDTH)_2]$ from the initial sulfur radical intermediate. Table III also includes the UV–vis spectral data for the $[M(TDT)_2]^-$ and $[M(TDT)_2]^{2-}$ complexes of Cu(II), Ni(II), Co(II), Fe(II), and Mn(II). The UV transitions that are observed between 200 and 400 nm are due to the ligand. The spectra for the $[M(TDT)_2]^-$ complexes contain an intense band in the visible region that is not observed for the $[M^{II}(TDT)_2]^{2-}$ complexes. The energy for these absorption bands is proportional to the ease of oxidation for the $M^{II}(TDT)_2^{2-}$ complex (Table II); the easier the removal of an electron the more negative the oxidation potential.

Table IV. Magnetic Moments for $[M(TDT)_2]^-$ Complexes in Dimethyl Sulfoxide

metal (M)	μ, μ_B
Zn	
Cu	0
Ni	1.83
Co	3.16
Mn	5.2
Fe	3.87
	3.77, solid {$[Fe(TDT)_2][Bu_4N]$·pyr}
	1.96, solid $[Fe(TDT)_2]_2[Bu_4N]_2$, per ion

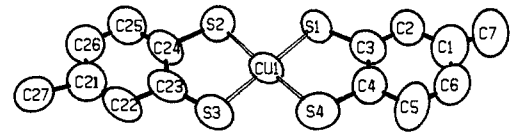

Figure 3. ORTEP diagram[47] for the X-ray crystal structure of $[CuTDT)_2][Bu_4N]$.

Magnetic Data. The solution magnetic moments for the $[M(TDT)_2]^-$ complexes are summarized in Table IV. Those for the solid complexes have been confirmed to be the same as previously reported.[35] The $[Cu(TDT)_2][Bu_4N]$ complex is diamagnetic over the temperature range from 6 to 300 K on the basis of SQUID measurements.

The solid dimeric $[Fe(TDT)_2]_2[Bu_4N]_2$ complex has a magnetic moment of 1.96 μ_B per iron and an apparent spin state of $^1/_2$ per iron. This changes to $S = {}^3/_2$ in the solid solution phase. We were unable to obtain accurate solution magnetic susceptibilities for $[M^{II}(TDT)_2]^{2-}$ complexes due to their sensitivity to oxygen and their low solubility in most electrochemical solvents.

X-ray Crystallography. The heavy atom parameters for $Cu(TDT)_2^-$ and $[Fe(TDT)_2]_2^{2-}$ anions are summarized in Table V. These results confirm that the solid $[Bu_4N][Cu(TDT)_2]$ complex is mononuclear (Figure 3 and Table VIA). The copper center is surrounded by an essentially square-planar array of four sulfur atoms from two TDT ligands with an average Cu–S bond distance of 2.613(12) Å.

The dimeric $[Fe(TDT)_2]_2[Bu_4N]_2$ complex has a roughly square-planar, but tetrahedrally distorted, arrangement of four thiolato sulfur atoms about the iron with an average Fe–S distance of 2.221 (6) Å (Figure 4 and Table VIB). The iron atom is displaced 0.38 Å out of the sulfur plane toward a fifth sulfur atom 2.51 (5) Å away in a second $Fe(TDT)_2^-$ ion across an inversion center. The Fe–Fe distance across this center is 3.252 (4) Å, too long to be significant. The two dithiolate ligands are individually planar within 0.04 Å, essentially experimental error, and have a dihedral angle of 163°. The coordination of S(3) to a second iron

(35) Williams, R.; Billig, E.; Waters, J. H.; Gray, H. B. *J. Am. Chem. Soc.* **1966**, *88*, 43.

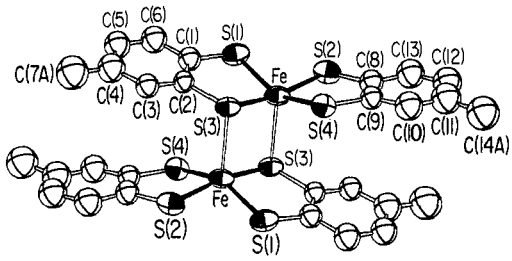

Figure 4. ORTEP diagram[47] for the X-ray crystal structure of $[Fe(TDT)_2]_2[Bu_4N]_2$.

atom displaces it only 0.13 Å from the Fe–S(1)–C(1)–C(2) plane. The S–C and C–C distances in the ligands are normal, if allowance is made for the effects of large apparent thermal motion in the toluene methyl groups.

Discussion and Conclusions

A self-consistent set of redox reactions for the metal dithiolate complexes is given in Table VII. The oxidation potential of $[Zn^{II}(TDT)_2]^{2-}$ is +0.18 V vs. SCE as compared to −0.05 V for the free ligand, $TDTH^-$, which indicates that the coordinated TDT^{2-} groups of $[Zn(TDT)_2]^{2-}$ are more stable to oxidation than $TDTH^-$. When the TDT^{2-} ligands are bound to the other first-row transition metals, their oxidation is facilitated and occurs at much more negative potentials. The extent of this shift in potential for the oxidation of $M^{II}(TDT)_2^{2-}$ as compared to that for free $TDTH^-$ is a measure of the degree of stabilization for the oxidation product that is conferred by the metal center of the complex.

The oxidations of $[Zn^{II}(TDT)_2]^{2-}$ and $TDTH^-$ are irreversible due to rapid dimerization of the thiolate radicals that are formed and the subsequent dissociation and hydrolysis of $[Zn^{II}(TDT)_2]$ to free Zn(II) and $H_2(TDT)_2$. However, this oxidation becomes reversible when the ligand is bound to a first row transition metal that contains one or more unpaired d electrons. This implies that the thiolate radical that is formed is deterred from dimerization and is further stabilized by the presence of these unpaired d electrons for coupling and bond formation. In fact, this oxidized product, $[M(TDT)_2]^-$, is the most stable form for each of the complexes.

The stabilization is believed to be due to coupling between the sulfur radical and an unpaired d electron to form a covalent bond; the more negative the oxidation potential for $[M^{II}(TDT)_2]^{2-}$ the greater degree of stabilization and bond strength in the product, M^{II}–(·TDT)(TDT)$^-$. On this basis the order of M^{II}–(·TDT) bond strength is Fe (−0.90 V) > Co (−0.84 V) > Mn (−0.67 V) > Cu (−0.59 V) > Ni (−0.51 V).

The oxidation potentials for the $(M^{II}Cl_4)^{2-}$ complexes are compared with those for the $[M^{II}(TDT)_2]^{2-}$ complexes in Table II. The first oxidation peak for the $(M^{II}Cl_4)^{2-}$ complexes occur in the range of +1.00 V vs. SCE (except for $(Fe^{II}Cl_4)^{2-}$) and is due to electron transfer from a bound chloride. The $(Fe^{II}Cl_4)^{2-}$ complex has a metal-centered reversible redox couple at +0.10 V to yield $(Fe^{III}Cl_4)^-$. For the other chloro complexes the metal (II/III) oxidation is not observed until well past +1.2 V.

The first oxidation peak for the $[M^{II}(TDT)_2]^{2-}$ complexes (dianions like the $(M^{II}Cl_4)^{2-}$ complexes) occurs at much more negative potentials (in the range from −0.47 to −0.83 V vs. SCE). This enhanced susceptibility to oxidation reflects the electron-donating capability of the thiolate ligands and is consistent with a ligand-centered electron transfer.

For the analogous 3,5-di-*tert*-butylcatechol ($DTBCH_2$) complexes, the initial redox chemistry is entirely ligand based and yields metal–semiquinonato complexes.[20-29] Although sulfur donors are related to oxygen donors, thiolates are much more susceptible to oxidation than are phenolates. To assign the initial oxidation for the $[M^{II}TDT)_2]^{2-}$ complexes to their metal center would be unreasonable when the analogous metal–catechol complexes undergo a ligand-based electron transfer. Furthermore, sulfur has vacant d orbitals that can accommodate electron density to result in a more positive metal center. Although the extent of this effect is speculative, a ligand-based oxidation is more favored than it is for complexes that contain oxygen donors.

Table V. Heavy Atom Parameters for the $Cu(TDT)_2^-$ and $[Fe(TDT)_2]_2^{2-}$ Anions

atom	x	y	z	B (Å²)
		A. $Cu(TDT)_2^-$		
Cu(1)	0.8750 (1)	−0.0115 (5)	0.0301 (2)	7.26 (9)
S(1)	0.8753 (2)	0.021 (1)	0.1439 (4)	7.6 (2)
S(2)	0.9244 (2)	0.088 (1)	0.0602 (5)	3.82
S(3)	0.8775 (3)	−0.055 (1)	−0.0826 (5)	9.1 (3)
S(4)	0.8260 (3)	−0.102 (1)	0.0025 (6)	10.4 (3)
N(1)	0.3746 (5)	−0.007 (3)	0.262 (1)	5.7 (5)
Ca(1)[a]	0.3850 (7)	0.097 (3)	0.206 (1)	6.5 (7)
Ca(2)	0.4018 (7)	0.000 (4)	0.157 (1)	8.3 (7)
Ca(3)	0.4115 (9)	0.121 (4)	0.100 (2)	10.1 (9)
Ca(4)	0.4299 (8)	0.047 (5)	0.053 (2)	13 (1)
Ca(5)	0.3487 (7)	−0.126 (3)	0.223 (1)	6.3 (7)
Ca(6)	0.3160 (7)	−0.041 (3)	0.173 (2)	7.8 (8)
Ca(7)	0.2917 (7)	−0.174 (4)	0.142 (1)	7.1 (8)
Ca(8)	0.2595 (9)	−0.095 (4)	0.090 (2)	10 (1)
Ca(9)	0.3633 (7)	0.107 (3)	0.312 (1)	5.8 (7)
Ca(10)	0.3488 (7)	0.020 (4)	0.369 (1)	7.5 (7)
Ca(11)	0.3387 (9)	0.154 (4)	0.416 (2)	11 (1)
Ca(12)	0.3218 (9)	0.096 (4)	0.467 (2)	11 (1)
Ca(13)	0.4025 (7)	−0.117 (3)	0.307 (1)	5.1 (6)
Ca(14)	0.4309 (7)	−0.016 (4)	0.352 (2)	7.3 (7)
Ca(15)	0.4610 (8)	−0.128 (4)	0.384 (2)	9.1 (9)
Ca(16)	0.4772 (9)	−0.177 (5)	0.322 (2)	11 (1)
C(1)	0.7958 (8)	−0.080 (4)	0.216 (4)	11 (1)
C(2)	0.8274 (7)	−0.032 (3)	0.215 (2)	8.3 (8)
C(3)	0.8367 (8)	−0.036 (3)	0.148 (2)	7.5 (8)
C(4)	0.8146 (8)	−0.094 (3)	0.086 (2)	8.2 (8)
C(5)	0.7819 (9)	−0.144 (4)	0.085 (2)	11 (1)
C(6)	0.7745 (8)	−0.138 (4)	0.153 (2)	9.6 (9)
C(7′)	0.784 (2)	−0.08 (1)	0.275 (4)	12 (2)
C(7)	0.742 (1)	−0.179 (8)	0.169 (4)	10 (2)
C(21)	0.9521 (9)	0.086 (4)	−0.154 (2)	10 (1)
C(22)	0.9225 (8)	0.024 (4)	−0.157 (2)	9.0 (9)
C(23)	0.9121 (8)	0.026 (4)	−0.089 (2)	8.8 (8)
C(24)	0.9361 (8)	0.085 (4)	−0.026 (2)	8.1 (8)
C(25)	0.9673 (8)	0.146 (4)	−0.026 (2)	10 (1)
C(26)	0.9753 (9)	0.147 (4)	−0.096 (2)	10 (1)
C(27)	0.968 (2)	0.101 (8)	−0.221 (4)	10 (2)
C(27′)	1.004 (2)	0.201 (9)	−0.106 (3)	10 (2)
		B. $[Fe(TDT)_2]_2^{2-}$		
Fe	0.5049 (2)	0.4242 (2)	0.5728 (2)	0.084 (1)[b]
S(1)	0.5036 (4)	0.2877 (3)	0.5086 (4)	0.103 (2)[b]
S(2)	0.4112 (4)	0.3565 (4)	0.6316 (3)	0.105 (2)[b]
S(3)	0.6211 (3)	0.4748 (3)	0.5315 (3)	0.084 (2)[b]
S(4)	0.5625 (3)	0.5179 (3)	0.6835 (3)	0.096 (2)[b]
C(1)	0.5180 (14)	0.3018 (16)	0.4569 (12)	7.5 (5)
C(2)	0.6353 (13)	0.3827 (13)	0.4647 (10)	6.4 (5)
C(3)	0.6988 (13)	0.3969 (13)	0.4257 (12)	7.8 (5)
C(4)	0.7082 (18)	0.3277 (19)	0.3682 (15)	11.1 (7)
C(5)	0.6550 (17)	0.2461 (19)	0.3611 (15)	10.0 (6)
C(6)	0.5955 (16)	0.2312 (15)	0.4039 (14)	10.0 (6)
C(7A)[c]	0.7740 (25)	0.3420 (22)	0.3258 (20)	15.0
C(7B)[c]	0.6568 (79)	0.1936 (79)	0.2948 (77)	15.0
C(8)	0.4221 (15)	0.4246 (15)	0.7165 (13)	8.2 (5)
C(9)	0.4879 (13)	0.4980 (14)	0.7415 (12)	7.2 (5)
C(10)	0.4983 (15)	0.5539 (15)	0.8123 (15)	11.0 (7)
C(11)	0.4404 (20)	0.5349 (22)	0.8574 (17)	12.9 (8)
C(12)	0.3761 (18)	0.4624 (19)	0.8370 (17)	12.0 (7)
C(13)	0.3702 (15)	0.4079 (15)	0.7691 (16)	11.1 (7)
C(14A)[d]	0.4388 (27)	0.5997 (29)	0.9185 (25)	15.0
C(14B)[d]	0.3162 (43)	0.4437 (42)	0.8852 (41)	15.0

[a] Anisotropically refined atoms are given in the form of the isotropic equivalent thermal parameter defined as: $(^4/_3)*[a2*B(1,1) + b2*B(2,2) + c2*B(3,3) + ab(\cos\gamma)*B(1,2) + ac(\cos\beta)*B(1,3) + bc(\cos\alpha)*B(2,3)]$. [b] U_{eq}. [c] Population C(7A) = 0.78 (2); C(7B) = 1–0.78. [d] Population C(14A) = 0.62 (2); C(14B) = 1–0.62.

Table VIII lists redox potentials for several copper(III) complexes with oxo and deprotonated amide donor groups, each of which is more positive than +0.4 V. In contrast, the ligand-based oxidations for $[Cu^{II}(DTBC)_2]^{2-}$ and $[Cu^{II}(TDT)_2]^{2-}$ occur at −0.53 and −0.59 V, respectively, to yield $[Cu^{II}(\cdot DTBSQ)(DTBC)]^-$ and $[Cu^{II}(\cdot TDT)(TDT)]^-$. The difference of 60 mV between the

Table VI. Selected Distances and Angles for the $Cu(TDT)_2^-$ and $[Fe(TDT)_2]_2^{2-}$ Anions[a]

atom	atom	dist (Å)	atom	atom	atom	angle (deg)
			A. $Cu(TDT)_2^-$			
Cu	S(1)	2.145 (9)	S(1)	Cu	S(2)	86.8 (4)
Cu	S(2)	2.190 (11)	S(1)	Cu	S(3)	176.1 (4)
Cu	S(3)	2.173 (11)	S(1)	Cu	S(4)	91.8 (4)
Cu	S(4)	2.149 (12)	S(2)	Cu	S(3)	91.4 (4)
S(1)	C(3)	1.73 (3)	S(2)	Cu	S(4)	178.0 (5)
S(2)	C(24)	1.81 (3)	S(3)	Cu	S(4)	90.0 (4)
S(3)	C(23)	1.66 (4)	Cu	S(1)	C(3)	105 (1)
S(4)	C(4)	1.76 (4)	Cu	S(2)	C(24)	104 (1)
			Cu	S(3)	C(23)	106 (1)
			Cu	S(4)	C(4)	105 (1)
			B. $[Fe(TDT)_2]_2^{2-}$			
Fe	S(1)	2.219 (6)	S(1)	Fe	S(3)	89.3 (2)
Fe	S(2)	2.224 (6)	S(2)	Fe	S(4)	88.9 (2)
Fe	S(3)	2.226 (5)	Fe	S(1)	C(1)	105.8 (8)
Fe	S(4)	2.213 (6)	Fe	S(2)	C(8)	105.4 (8)
S(1)	C(1)	1.71 (2)	Fe	S(3)	C(2)	105.0 (6)
S(3)	C(2)	1.80 (2)	Fe	S(4)	C(9)	105.0 (7)
S(2)	C(8)	1.70 (2)				
S(4)	C(9)	1.77 (2)				

[a] C–C (benzene rings) 1.39 (3) average.

complexes with S and O donors reflects the increased stabilization of the RS· radical by the unpaired d electron as compared to that of the RO· radical.

The ^{13}C NMR spectrum of the $[Cu(TDT)_2]^-$ complex contains a unique resonance at 142.6 ppm, which has been assigned to the carbon bonded to a ligand sulfur radical.[45] A similar resonance is observed at 134.2 ppm for the C-4 carbon of the disulfide-bridged dimeric product $H_2(TDT)_2$ (from electrooxidation of $TDTH^-$) and is absent in the spectrum for $TDTH_2$ and $TDTH^-$. The difference of 8.4 ppm probably is due to the difference between a disulfide (sulfur radical–sulfur radical) and a metal d^n–(·SR) bond.

The optical spectra for $[M^{II}(TDT)_2]^-$ complexes contain a unique electronic band that is absent in the spectra of their reduced counterparts, $[M^{II}(TDT)_2]^{2-}$. The energies for this absorption band [Fe(19 000 cm^{-1}); Cu (8 100 cm^{-1})] are in general accord with the relative M^{II}–(·TDT) bond stabilities that are indicated by the negative shifts in the oxidation potentials for the $[M^{II}(TDT)_2]^{2-}$ complexes (Table II). A reasonable conclusion is that the band is due to excitation of the sulfur radical electron in the M^{II}–(·TDT) bond; the greater the bond stability the greater the excitation energy.

Reference to Table VI confirms that the four metal–sulfur bond distances in the $Cu(TDT)_2^-$ complexes and in the $[Fe(TDT)_2]_2^{2-}$ complex are equal within experimental error. The structures do not distinguish between the two types of bonding that are proposed (three metal–thiolate coordination bonds and one metal d^n–(·SR) covalent bond). The molecular structure of $[Fe(TDT)_2]_2^{2-}$ is similar to that of the dimeric $[Co(S_2C_6Cl_4)_2]_2^{2-}$ complex.[46] With a square-pyramidal Co complex the metal Co atom is raised 0.26 Å out of the place of the four basal S atoms as compared to 0.38 Å out-of-plane displacement for the Fe atom in the $[Fe(TDT)_2]_2^{2-}$ complex. The similarities in the two structures indicate analogous bonding and imply the involvement of the same d orbital to form a unique bond with the sulfur radical.

The solution magnetic moments for the $[M(TDT)_2]^-$ complexes agree well with those for the solids (except for $[Fe(TDT)_2]^-$) (Table III). The monomeric, five-coordinate pyridine adduct, $[Fe^{II}(TDT)_2(py)][Bu_4N]$, has a spin state of $^3/_2$ for the solid and in solution. The dimeric complex $[Fe^{II}(TDT)_2]_2[Bu_4N]_2$, on the other hand, has an apparent spin state of $^1/_2$ per iron in the solid phase, but in the solution phase $S = {}^3/_2$ per iron. The decreased moment has been attributed to spin-coupling between the two iron atoms in the solid phase, but the exact nature of this coupling mechanism is not understood. The scope of this work mainly involves solution chemistry and both complexes are confirmed to be monomeric, $S = {}^3/_2$ systems under these conditions.

The magnetic moments for the $[M(TDT)_2]^-$ complexes in Table IV are consistent with either low-spin or intermediate-spin trivalent metal-centered coordination complexes or, more reasonably, a divalent metal with one of its unpaired d electrons spin-coupled to a sulfur radical. For $[Fe(TDT)_2]^-$ ($S = {}^3/_2$), an intermediate spin iron(III) ion must be proposed to adequately sustain the argument of a metal-centered oxidation. For all of the $[M^{II}(TDT)_2]^{2-}$ complexes, the issue of a metal-centered or ligand-centered oxidation cannot be resolved on the basis of the magnetic data alone. However, the redox potential for the $Fe^{III}Cl_4^-/Fe^{II}Cl_4^{2-}$ couple is by far the most negative of the chloro complexes (Table II), and if oxidation of $Fe^{II}(TDT)_2^{2-}$ is ligand centered, then that will be the case of the other $[M^{II}(TDT)_2]^{2-}$ complexes. For the $[Fe^{II}(TDT)_2]^{2-}$ complex, a metal-centered oxidation of high spin iron(II) ($S = {}^4/_2$) would result in high spin iron(III) with $S = {}^5/_2$, but a ligand-centered oxidation with the sulfur-radical product spinpaired with one of the unpaired d electrons of high spin iron(II) would give an $S = {}^3/_2$ system, as is observed. Intermediate spin states for iron(III) porphyrins have been reported,[41,42] but such an iron(III) spin state for $[Fe(TDT)_2]^-$ is unreasonable on the basis of the electrochemical, spectroscopic, and magnetic data of Tables II–IV and VII.

The question of the site of electron transfer and subsequent assignment of formal oxidation states for the $[M(TDT)_2]^-$ complexes may appear to be more semantic than chemical. However,

(36) Henkel, G.; Greiwe, K.; Krebs, B. *Angew. Chem., Int. Ed. Engl.* **1985**, *24*, 117.
(37) Margerum, D. W.; Chellappa, K. L.; Bossu, F. P.; Bruce, G. L. *J. Am. Chem. Soc.* **1975**, *97*, 6894.
(38) Bour, J. J.; Birkner, P. J. M.; Steggerda, J. J. *Inorg. Chem.* **1971**, *10*, 1202.
(39) Levitski, A.; Anbar, M.; Berger, A. *Biochemistry* **1967**, *6*, 3757.
(40) Dyrkacz, G. R.; Libby, R. D.; Hamilton, G. A. *J. Am. Chem. Soc.* **1976**, *98*, 626.
(41) Reed, C. A.; Mashiko, T.; Bentley, S. P.; Kastner, M. E.; Scheidt, W.R.; Spartalian, K.; Lang, G. *J. Am. Chem. Soc.* **1979**, *101*, 2948.
(42) Masuda, H.; Taga, T.; Osaki, K.; Sugimoto, H.; Yoshida, Z. I.; Ogoshi, H. *Inorg. Chem* **1980**, *19*, 950.
(43) Groves, J. T.; Haushalter, R. C.; Nakamura, M.; Nemo, T. E.; Evans, B. J. *J. Am. Chem. Soc.* **1981**, *103*, 2884.
(44) Jones, S. E.; Srivatsa, G. S.; Sawyer, D. T.; Traylor, T. G.; Mincey, T. C. *Inorg. Chem.* **1983**, *22*, 1983.
(45) Sabat, M.; Bodini, M. E.; Srivatsa, G. S.; Sawyer, D. T. *J. Spanish Roy. Chem. Soc.*, in press.
(46) Baker-Hawkes, M. J.; Dori, Z.; Eisenberg, R.; Gray, H. B. *J. Am. Chem. Soc.* **1968**, *90*, 4253.

Table VII. Redox Reactions for the $M^{II}TDT$ Complexes in MeCN (0.1 M TEAP)

$TDTH_2$:

$$TDTH_2 + e^- \xrightarrow{-1.02\ V\ vs.\ SCE} TDTH^- + {}^1/_2H_2$$

$$2TDTH^- \xrightarrow{-0.05\ V} 2TDTH\cdot + 2e^-$$

$$\downarrow$$

$$H_2(TDT)_2$$

$$TDTH^- + OH^- \xrightarrow{-0.06\ V} TDT^{-}\cdot + H_2O + e^-$$

$$\downarrow H_2O$$

$${}^1/_2H_2(TDT)_2 + OH^-$$

$Zn^{II}(TDT)_2^{2-}$:

$$Zn^{II}(TDT)_2^{2-} \xrightarrow{+0.18\ V} Zn^{II}[(TDT)_2] + 2e^-$$

$$\downarrow H_2O$$

$$Zn(II) + H_2(TDT)_2 + 2OH^-$$

$Cu^{II}(TDT)_2^{2-}$:

$$Cu^{II}(TDT)_2^{2-} + e^- \underset{}{\overset{-1.48\ V}{\rightleftharpoons}} Cu^{I}(TDT)_2^{3-}$$

$$Cu^{I}(TDT)_2^{3-} \xrightarrow{H_2O} Cu^{II}(TDT)_2^{2-} + {}^1/_2H_2 + OH^-$$

$$\xrightarrow{H_2O} Cu^{I}(TDT)^- + TDTH^- + OH^-$$

$$Cu^{II}(TDT)_2^{2-} \overset{-0.59\ V}{\rightleftharpoons} {}^{II}(\cdot TDT)(TDT)^- + e^-$$

$$Cu^{II}(\cdot TDT)(TDT)^- \xrightarrow{+0.62\ V} Cu(II) + {}^1/_n(TDT\text{–}TDT)_n + 3e^-$$

$Ni^{II}(TDT)_2^{2-}$:

$$Ni^{II}(TDT)_2^{2-} \overset{-0.51\ V}{\rightleftharpoons} Ni^{II}(\cdot TDT)(TDT)^- + e^-$$

$$Ni^{II}(\cdot TDT)(TDT)^- \underset{+0.28\ V}{\overset{+0.42\ V}{\rightleftharpoons}} Ni^{III}(\cdot TDT)(TDT) + e^-$$

$Co^{II}(TDT)_2^{2-}$:

$$Co^{II}(TDT)_2^{2-} \overset{-0.84\ V}{\rightleftharpoons} Co^{II}(\cdot TDT)(TDT)^- + e^-$$

$$Co^{II}(\cdot TDT)(TDT)^- \xrightarrow{+0.20\ V} Co^{III}(\cdot TDT)(TDT) + e^-$$

$Fe^{II}(TDT)_2^{2-}$:

$$Fe^{II}(TDT)_2^{2-} \overset{-0.90\ V}{\rightleftharpoons} Fe^{II}(\cdot TDT)(TDT)^- + e^-$$

$$2Fe^{II}(\cdot TDT)(TDT)^- \overset{+0.10\ V}{\rightleftharpoons} [Fe^{III}(\cdot TDT)(TDT)Fe^{II}(\cdot TDT)(TDT)]^- + e^-$$

$$\downarrow\uparrow +0.32\ V$$

$$[Fe^{III}(\cdot TDT)(TDT)Fe^{III}(\cdot TDT)(TDT)] + e^-$$

$$\downarrow +1.00\ V$$

$$2Fe(II) + {}^2/_n(TDT\text{–}TDT)_n + 4e^-$$

$$\downarrow 8e^-,\ -0.93\ V$$

$$2Fe^{II}(TDT)_2^{2-}$$

$Mn^{II}(TDT)_2^{2-}$:

$$Mn^{II}(TDT)_2^{2-} \overset{-0.67}{\rightleftharpoons} Mn^{II}(\cdot TDT)(TDT)^- + e^-$$

$$Mn^{II}(\cdot TDT)(TDT)^- \xrightarrow{+0.22\ V} Mn^{II} + {}^1/_n(TDT\text{–}TDT)_n + 3e^-$$

their redox chemistry is much more consistent with a common redox-active ligand than with a metal-centered electron transfer. The standard redox potentials for the M(III/II) couples range from +0.77 vs. NHE for Fe(III) to +1.8 V for Co(III), but the reduction potentials for the $[Fe^{II}(TDT)_2]^-$ and $[Co^{II}(TDT)_2]^-$ complexes are within 0.06 V of each other (Table VII).

VIII. Reduction Potentials for Several Copper(III) and Copper(II) (Radical-Ligand) Complexes

complexes	redox potent. (V vs. SCE)	ref
A. Copper(III)		
H_{-2} triglycine	+0.92	37
biuret	+0.89	38
H_{-3} tetraglycine	+0.61	37
H_{-3} tetraalanine	+0.58	39
galactose oxidase	+0.42	40
B. Copper(II)–(Radical Ligand)		
$[Cu^{II}(DTBSQ)(DTBC)]^-/[Cu^{II}(DTBC)_2]^{2-}$	−0.53	29
$[Cu^{II}(TDT)_2]^-/[Cu^{II}(TDT)_2]^{2-}$	−0.59	this work

The ESR studies of oxidized metal–dithiolate complexes[48,49] been interpreted to be due to appreciable mixing of unpaired spin in metal d orbitals and ligand donor orbitals. This is consistent with the proposed bonding for the present oxidized metal–dithiolate complexes $[M(TDT)_2^-]$. However, characterization of the final oxidized state of an electron transfer process does not provide any insight as to the site of electron removal for the initial reduced state.

Highly oxidized metal centers have been proposed as intermediates in the chemistry of cytochrome P-450,[43] which contains an axial thiolate ligand. In such systems, the possibility that the thiolate ligand participates in the redox chemistry is a viable alternative to invocation of exotic oxidation states such as Fe(IV) and Fe(V), which involve the stabilization of a highly electropositive iron center bound to a strongly reducing thiolate ion. Future studies will be directed to iron porphyrin models that incorporate a thiolate ligand that is covalently bound to porphyrin ring.[44] Detailed characterization of the oxidation product of such a model in the absence and presence of dioxygen and hydrogen peroxide will give new insights into the nature of the reactive intermediates of cytochrome P-450.

Acknowledgment. This work was supported by National Science Foundation under Grants No. CHE 821229 (D.T.S.) and INT-8212234 (D.T.S.) and by the Exxon Education Foundation (W.P.S.).

Registry No. $TDTH_2$, 496-74-2; $TDTH^-$, 99923-32-7; $H_2(TDT)_2$, 99903-39-6; $[Cu(TDT)_2][Bu_4N]$, 15551-24-3; $[Fe(TDT)_2][Bu_4N]$, 21370-26-3; $[Zn^{II}(TDT)_2]^{2-}$, 99923-31-6; $[Mn^{II}(TDT)_2]^{2-}$, 94595-52-5; $[Cu^{II}(TDT)_2]^{2-}$, 46944-69-8; $[Ni^{II}(TDT)_2]^{2-}$, 46944-71-2; $[Co^{II}(TDT)_2]^{2-}$, 46944-95-0; $[Fe^{II}(TDT)_2]^{2-}$, 46944-98-3; $[Ni^{II}(TDT)_2]^{1-}$, 13964-76-6; $[Co^{II}(TDT)_2]^-$, 14874-45-4; $[Mn^{II}(TDT)_2]^-$, 94500-28-4.

Supplementary Material Available: Tables of cation parameters, anisotropic thermal parameters, hydrogen parameters, and structure factors for both structures (22 pages). Ordering information is given on any current masthead page.

(47) Johnson, C. K. ORTEP, Report ORNL-5138, Oak Ridge National Laboratory, TN, 1965.

(48) Maki, A. H.; Edelstein, N.; Davison, A.; Holm, R. H. *J. Am. Chem. Soc.* **1964**, *86*, 4581.

(49) Kirmse, R.; Dietzsch, W. *J. Inorg. Nucl. Chem.* **1976**, *38*, 255 and references therein.